Am J Physiol Renal Physiol 305: F1365–F1373, 2013.
First published July 17, 2013; doi:10.1152/ajprenal.00009.2013.

The inhibitory effect of $G_{\beta\gamma}$ and G_{β} isoform specificity on ENaC activity

Ling Yu,[1,2,3] Otor Al-Khalili,[1,2] Billie Jeanne Duke,[1] James D. Stockand,[4] Douglas C. Eaton,[1,2] and Hui-Fang Bao[1,2]

[1]*Department of Physiology, Emory University School of Medicine, Atlanta, Georgia;* [2]*The Center for Cell and Molecular Signaling, Emory University School of Medicine, Atlanta, Georgia;* [3]*College of Resources and Environmental Sciences, Nanjing Agricultural University, Nanjing, China; and* [4]*Department of Physiology, University of Texas Health Science Center, San Antonio, Texas*

Submitted 7 January 2013; accepted in final form 26 June 2013

Yu L, Al-Khalili O, Duke BJ, Stockand JD, Eaton DC, Bao H-F. The inhibitory effect of $G_{\beta\gamma}$ and G_{β} isoform specificity on ENaC activity. *Am J Physiol Renal Physiol* 305: F1365–F1373, 2013. First published July 17, 2013; doi:10.1152/ajprenal.00009.2013.—Epithelial Na^+ channel (ENaC) activity, which determines the rate of renal Na^+ reabsorption, can be regulated by G protein-coupled receptors. Regulation of ENaC by Gα-mediated downstream effectors has been studied extensively, but the effect of $G_{\beta\gamma}$ dimers on ENaC is unclear. A6 cells endogenously contain high levels of $G_{\beta1}$ but low levels of $G_{\beta3}$, $G_{\beta4}$, and $G_{\beta5}$ were detected by Q-PCR. We tested $G\gamma_2$ combined individually with $G_{\beta1}$ through $G_{\beta5}$ expressed in A6 cells, after which we recorded single-channel ENaC activity. Among the five β and γ_2 combinations, $\beta_1\gamma_2$ strongly inhibits ENaC activity by reducing both ENaC channel number (*N*) and open probability (P_o) compared with control cells. In contrast, the other four β-isoforms combined with γ_2 have no significant effect on ENaC activity. By using various inhibitors to probe $G_{\beta1\gamma2}$ effects on ENaC regulation, we found that $G_{\beta1\gamma2}$-mediated ENaC inhibition involved activation of phospholipase C-β and its enzymatic products that induce protein kinase C and ERK1/2 signaling pathways.

G protein βγ subunits; ENaC; phospholipase C; protein kinase C; single channels

EPITHELIAL NA CHANNELS (ENaC) are sodium-permeable ion channels located in the apical membrane of polarized epithelial cells primarily in the distal nephron, lung, and distal colon. In the distal nephron, the activity of ENaC is the rate-limiting step for Na^+ reabsorption (17, 57); therefore, ENaC activity is critical in the physiological maintenance of systemic Na^+ homeostasis and long-term control of blood pressure. Because of its central role in responding to changes in Na^+ uptake, ENaC activity is tightly regulated; abnormal regulation of this channel has been linked to several genetic disorders involving abnormal blood pressure including Liddle's syndrome and pseudohypoaldosteronism type 1. ENaC is regulated by many intracellular as well as extracellular factors, among these G protein-coupled receptors (GPCRs), which transduce a variety of extracellular signals to several different intracellular signaling pathways that have been implicated in ENaC regulation. Trimeric G proteins are a family of 40- to 50-kDa proteins that each consist of three subunits: one α, one β, and one γ. Ligand binding to a GPCR leads to a series of events. First, GDP bound to the α subunit is replaced with GTP, after which the α subunit dissociates from the βγ subunits. The βγ subunits remain tightly associated with each other and remain anchored in the membrane via myristoylation of the γ subunit. Generally, the immediate GPCR signal is mediated by the intracellular association of the GTP-bound G_{α} with signaling molecules that are subsequently activated. α Subunits fall into many different categories. The most common are stimulators of adenylyl cyclase, $G_{\alpha s}$, inhibitors of adenylyl cyclase, $G_{\alpha i}$, and activators of phospholipase C, $G_{\alpha q}$. Several GPCRs alter ENaC activity after interacting with their ligands. Vasopressin (8, 13), β-adrenergic agents, dopamine, purines, adenosine, angiotensin II, endothelin, and many others all activate GPCRs, and the activated α-subunits modulate ENaC activity. Occasionally, G protein α subunits interact directly with effector proteins including ENaC rather than first interacting with signaling intermediates (1, 16, 32, 50–52, 69).

All of these G protein effects are mediated by the release of the G protein α subunits, but in every case a βγ dimer is also released. In some circumstances, GPCR effects coupled to Gi/o signaling are mediated by $G_{\beta\gamma}$ (18); however, there are few descriptions of the effects of βγ dimers on ENaC regulation. $G_{\beta\gamma}$ might inhibit ENaC activity through several downstream events. $G_{\beta\gamma}$ can stimulate phospholipase C-β isoforms (PLC-β) and promote phosphorylation of PLC-γ, which can, in turn, hydrolyze phosphatidylinositol 4,5-bisphosphate {[PI(4,5)P(2)]; PIP_2} and generate the second messengers: inositol 1,4,5-trisphosphate (IP_3) and diacylglycerol (DAG). PIP_2 is essential for ENaC gating (33, 44, 69) so that hydrolysis will reduce ENaC activity while the hydrolysis products, IP_3 and DAG, may further activate PKC and thereby inhibit ENaC open probability (P_o) and surface expression (6, 28). $G_{\beta\gamma}$ may also trans-activate receptor tyrosine kinases such as EGFR or TGFR (39, 56), after which these receptors initiate signaling cascades that inhibit ENaC activity (19, 37, 61).

In the human genome, there are 5 G_{β} and 12 G_{γ} isoforms as well as two additional β splice variants. The β subunits all have high sequence identity: β1 through β4 have 78–88% amino identity (24), and β_5 is ~50% identical to other β subunits (64). In contrast, all γ subunits are more diverse, ranging from 27 to 76% amino acid identity; therefore, the signaling specificity of $G_{\beta\gamma}$ was assumed to be based on the γ subunits (12, 30, 49). However, recent research shows that, in fact, β subunits determine the effector specificity (26, 27, 47). Most G_{β} and G_{γ} subunits can form dimers in vitro, but in vivo studies have indicated that there are preferential associations for different $G_{\beta\gamma}$ subunits in living cells, and these preferential associations may play an important role in determining the signaling specificity (46).

To address the effect of $G_{\beta\gamma}$, particularly the specificity of β isoforms, on ENaC regulation, we examined the effect of combinations of β1 through β5 with γ_2 on endogenous ENaC

Address for reprint requests and other correspondence: L. Yu, College of Resources and Environmental Sciences, Nanjing Agricultural Univ., Nanjing 210095, China (e-mail: lyu@njau.edu.cn).

Table 1. *Quantitative PCR primers for Xenopus laevis G_β subunits*

Subunit	GenBank	Forward Primer	Reverse Primer	Threshold Cycle Number
β1	XLGNB1	CCACTTTGGCTCAGATCACA	CAGAGGAATGGCATGAACCT	22.9 ± 1.49
β2	XLGNB2	CCACACTGGCTACCTGAACA	TTGCTGCTGGTGCTGATAAC	40.0 ± 0.00
β3	XLGNB3	CCAGCTCAGGAGACACAACA	GCAAGTCAAACATGCGACAC	32.0 ± 2.49
β4	XLGNB4	CCAGGCCACACAGGTTACTT	GAAGCATCACAAGCACCAGA	24.7 ± 1.31
β5	XLGNB5	TTCACCACCAACAAGGAACA	AGCTGCAGGCAGAGAGGTAG	29.3 ± 0.49

Values are means ± SD. All primers were validated by melt curve analysis of subunit-containing plasmids.

in A6 cells, a *Xenopus laevis* kidney cell line. The γ_2 subunit was chosen because dimers containing this isoform are active in most assays of βγ function (49). By using patch-clamp and single-channel recording, we show that only $\beta_1\gamma_2$ inhibits ENaC activity among these five combinations, and this inhibition is primarily mediated by $\beta_1\gamma_2$ activation of PLC and subsequent activation of PKC and ERK1/2.

METHODS

A6 cell culture and gene transfection. A6 cells were maintained in plastic tissue culture flasks at 26°C with 4% CO_2 in air; cells between *passages 97* and *104* were grown on permeable filters for patch-clamp recording (66). A6 cells were transfected with $G_{\gamma 2}$ (in pIRES2-DsRed-Express bicistronic vector) combined with different G_β (in pIRES2-EGFP bicistronic vector) with Lipofectamine 2000 transfection reagent (Invitrogen) at initial cell confluence.

Single-channel recordings. A6 cell single-channel recording was performed in cells expressing both green fluorescent protein (GFP) and red fluorescent protein (RFP) 4–7 days posttransfection. All experiments were carried out with cell-attached configuration. The bath and pipette solutions were the same, containing (in mM) 96 NaCl, 3.4 KCl, 0.8 $MgCl_2$, and 10 HEPES; pH 7.4. In general, cells were not exposed to patch-clamp solution for more than 2 h. The pipette holding potential ($-V_{pip}$) was 0 or −10 mV, and the recording duration was 8–10 min.

Drug treatments. The ERK1/2 kinase inhibitor U0126, PLC inhibitor U73122, and its inactive analog U73433 were obtained (Sigma), and all were dissolved in DMSO at 10 mM for stock and used as 10 μM; the PKC inhibitor GF109203X and Src family kinase inhibitor PP2 (Calbiochem) were prepared as 2 mM stocks in DMSO and finally used as 0.4 and 2 μM, respectively; the phosphatidylinositol 3-kinase (PI3K) inhibitor LY294002 (Cell Signaling) was dissolved in 10 mM DMSO and applied as 10 μM. Drugs were added to the bath solution at least 20 min before channel recording.

Real-time PCR. We recovered five Gβ sequences, β1–β5, from GenBank and developed multiple sets of potential primers for each subunit. We examined the melt curves for each primer and selected five pairs with the highest selectivity (given in Table 1). The lower detection limit with our PCR unit (Bio-Rad Icycler) was 40 cycles. All levels of expression were referenced to β2, which was not detected at <40 cycles. The efficiency of the PCR reaction was determined with a plasmid containing β1 as 1.96-fold/cycle, and fold-changes were calculated accordingly.

Data analysis. All data acquisition and analysis were performed as described previously (66). Data are reported as means ± SE. Statistical analysis was performed by SigmaPlot and SigmaStat software (Jandel Scientific). Differences between groups were evaluated with one-way ANOVA, and results were considered significant if $P < 0.05$.

RESULTS

Prior work has shown that βγ subunits can, under appropriate conditions, alter ENaC activity (69), but which β subunits are responsible for the effects was unclear.

G_β subunits in A6 cells. We used quantitative PCR to determine message levels for different G_β subunits. Primers were developed from GenBank sequences and tested for specificity using melt curve analysis. Relative amounts of message for different G_β subunits were calculated based on threshold cycle crossing. Figure 1 shows that the major subunit present on A6 cells is β1 with over 3.31 times more than β4, the next most common subunit. β1 is also over 75 times more prevalent than β5 and 465 greater than β3. β2 was not detectable (although the primers could easily amplify β2 present in plasmid DNA). We used Western blots to look for G_β protein.

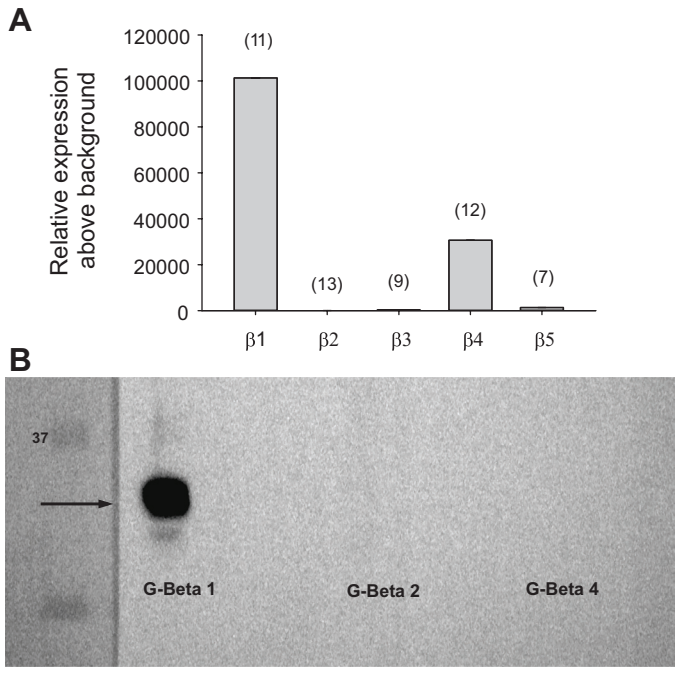

Fig. 1. G_β subunits in A6 cells. *A*. quantitative PCR to detect G_β subunits in A6 cells. Primers based on GenBank sequences for $G_{\beta 1-5}$ were selected on the basis of their melt curves (given in Table 1). The lower detection limit with our PCR unit (Bio-Rad Icycler) was 40 cycles. All levels of expression were referenced to β2, which was not detected at less than 40 cycles. Threshold cycles for each subunit are given in Table 1. The efficiency of the PCR was determined with a plasmid containing β1 as 1.96-fold per cycle, and fold-changes shown in this figure were calculated accordingly. Standard deviations for all subunits are too small to be visible in this plot. Every value is significantly different from every other value (ANOVA with Holm-Sidak posttest, $P < 0.05$). *B*: Western blots of G_β subunits in A6 cells. Whole lysate from 2F3 cells were probed with antibodies to $G_{\beta 1}$, $G_{\beta 2}$, and $G_{\beta 4}$. Antibodies were obtained from Santa Cruz Biotechnology. These subunits were chosen since they represent quite different levels of expression: β1, high; β2, undetectable; β4, very low, but detectable. Twenty-five micrograms of total protein was loaded in each lane with antibodies at 1:500. All secondary antibodies were used at 1:5,000. $G_{\beta 1}$ and $G_{\beta 2}$ used anti-rabbit secondary antibody, and $G_{\beta 4}$ used goat anti-mouse secondary antibody. $G_{\beta 1}$, $G_{\beta 2}$, and $G_{\beta 4}$ are expected to run between 35 and 37 kDa as does $G_{\beta 1}$. $G_{\beta 2}$ and $G_{\beta 4}$ are not detectable.

We chose β1, β2, and β4 as examples of a highly expressed, moderately expressed, and very poorly expressed subunit, respectively. Figure 1 shows that β1 is easily detected, but that the other two subunits are not detectable. This result suggested that the most likely G_β subunits to regulate ENaC in A6 cells would be β1, but β4, β3, or β5 might also be involved. (An examination by Western blotting of β subunits in another cell line that expresses ENaC, mpkCCD-I4 cells, showed the same subunits as A6 cells in the same proportion except that β2 was at levels comparable to β4; data not shown). We did not examine the prevalence of γ subunits since there are a large number of them, but the γ_2 subunit was chosen because dimers containing this isoform are active in most assays of βγ function and because it is common in most epithelia (49).

Effect of different $G_{\beta\gamma}$ combinations on ENaC activity. Transfection efficiency of A6 cells is low. To perform patch-clamp recording on cells expressing both G_β and G_γ subunits, G_β was inserted in the second cloning site of the bicistronic vector pIRES-GFP, which expresses GFP coordinately with the gene construct, while G_γ was inserted into the bicistronic vector pIRES-DsRED, which expresses RFP coordinately. Single-channel, cell-attached patches were only formed on cells that expressed both GFP and RFP, the reporter genes for G_β and G_γ, respectively. To eliminate variability in ENaC activity, which may arise among cells of different passages or even among cells on different days after gene transfection, control cells which only expressed reporter genes were always recorded in parallel with cells coexpressing $G_{\beta\gamma}$. The single-channel conductance of ENaC, regardless of which $G_{\beta\gamma}$ combination was expressed in cells, is ~4 pS, which is similar to that of ENaC in cells transfected with empty vectors; however, the five combinations do have different effects on ENaC activity (average channel activity; NP_o). In $G_{\beta1\gamma2}$-expressing cells, channel activity is significantly reduced, while other βγ combinations produced no significant effect on ENaC activity. Typical single-channel traces recorded from control and $G_{\beta1\gamma2}$-expressing cells are shown in Fig. 2*A*; the NP_o, channel number within a patch (N) and channel (P_o) of these two groups of cells are presented in Fig. 2, *B–D*. The NP_o of $G_{\beta1\gamma2}$-expressing cells is 0.07 ± 0.02 (n = 25), which is significantly lower than the control value of 0.39 ± 0.13 (n = 29), P = 0.003. To further analyze whether channel N and/or P_o is reduced by $G_{\beta1\gamma2}$, we estimated channel density (N) by counting the maximum level of unitary current. If the recording period is sufficiently long (usually >10 min) (45) and if P_o is between 0.1 and 0.9, N can be determined with >95% confidence. In our experiments, each patch was recorded for ~10 min, and therefore we should have reasonable estimates of channel N and also channel P_o by dividing NP_o by N. The channel density, N, is 1.12 ± 0.03 (n = 25) for $G_{\beta1\gamma2}$-expressing cells. This is significantly lower than control cells with an N of 2.34 ± 0.54 (n = 29) (P = 0.05) (Fig. 2*C*). In parallel with the decrease in N, P_o of $G_{\beta1\gamma2}$-expressing cells is 0.05 ± 0.01 (n = 11), which is also significantly reduced compared with its control value of 0.12 ± 0.02 (n = 18), P = 0.027 (Fig. 2*D*).

In the same way, we also examined the effect of $G_{\beta2}$–$G_{\beta5}$ combinations with $G_{\gamma2}$ on ENaC regulation. The average channel NP_o of these $G_{\beta\gamma}$-expressing cells is presented side by side with the average values from their respective controls (Fig. 3, *A–C*). NP_o of $G_{\beta2\gamma2}$-expressing cells is 0.17 ± 0.05 (n = 33) and that of its control is 0.15 ± 0.05 (n = 36); NP_o of $G_{\beta3\gamma2}$- and $G_{\beta4\gamma2}$-expressing cells is 0.12 ± 0.05 (n = 15) and 0.12 ± 0.03 (n = 31), and that of their control is 0.1 ± 0.03 (n = 33), respectively. Finally, NP_o of $G_{\beta5\gamma2}$-expressing cells is 0.11 ± 0.04 (n = 32), while that of its control is 0.07 ± 0.02 (n = 30). In contrast to the significant inhibitory effect of $G_{\beta1\gamma2}$ on ENaC activity, the rest of the four $G_{\beta\gamma}$ combinations have no significant effect on ENaC activity. We also analyzed functional ENaC surface density (N) and channel gating (P_o) of these cells, and we found that both parameters in control and these four $G_{\beta\gamma}$-expressing cells are similar (data not shown). There is often substantial variability of P_o for ENaC from different passages of cells and after different numbers of days in culture. In fact, single-channel activity of control cells recorded in parallel with any of these four $G_{\beta\gamma}$ (β2–β5)-expressing cells is low (NP_o of the control cells was <0.15). We speculated that the low P_o might disguise the effect of these $G_{\beta\gamma}$ subunits. Therefore, to further investigate the specificity of the $G_{\beta\gamma}$ effects, we reexamined $G_{\beta4\gamma2}$ and $G_{\beta5\gamma2}$ in cells with higher ENaC channel activity. Early-passage cells that are just confluent tend to have a higher P_o. We measured an ENaC NP_o of $G_{\beta4\gamma2}$- or $G_{\beta5\gamma2}$-expressing cells of 0.57 ± 0.12 (n = 23) and 0.50 ± 0.12 (n = 24), respectively, which even with the high initial P_o was again not significantly different from the NP_o of 0.59 ± 0.19 (n = 32) measured in control GFP- and RFP-expressing cells. This result implies that

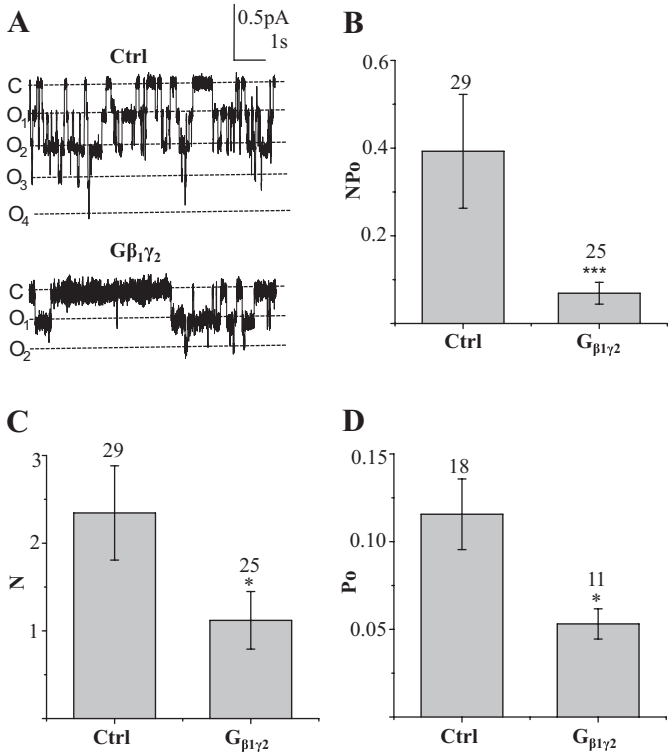

Fig. 2. $G_{\beta1\gamma2}$ inhibits ENaC activity of A6 cells. *A*: representative trace of single-channel records from green fluorescent protein (GFP)- and red fluorescent protein (RFP)-expressing cells (Control) and $G_{\beta1\gamma2}$-expressing cells. The closed state of the epithelial Na^+ channel (ENaC) is indicated with "c," and channel opening(s) are marked with "o." *B*: average channel activity (NP_o) values from these 2 groups of cells. *C* and *D*: averaged number (N) of channels within a patch and averaged channel open probability (P_o) are independently presented by first determining N and then dividing NP_o by N within each patch for the P_o values. The number indicated on top of each column is number of successful patches. Values are means ± SE. *P < 0.05, ***P < 0.01.

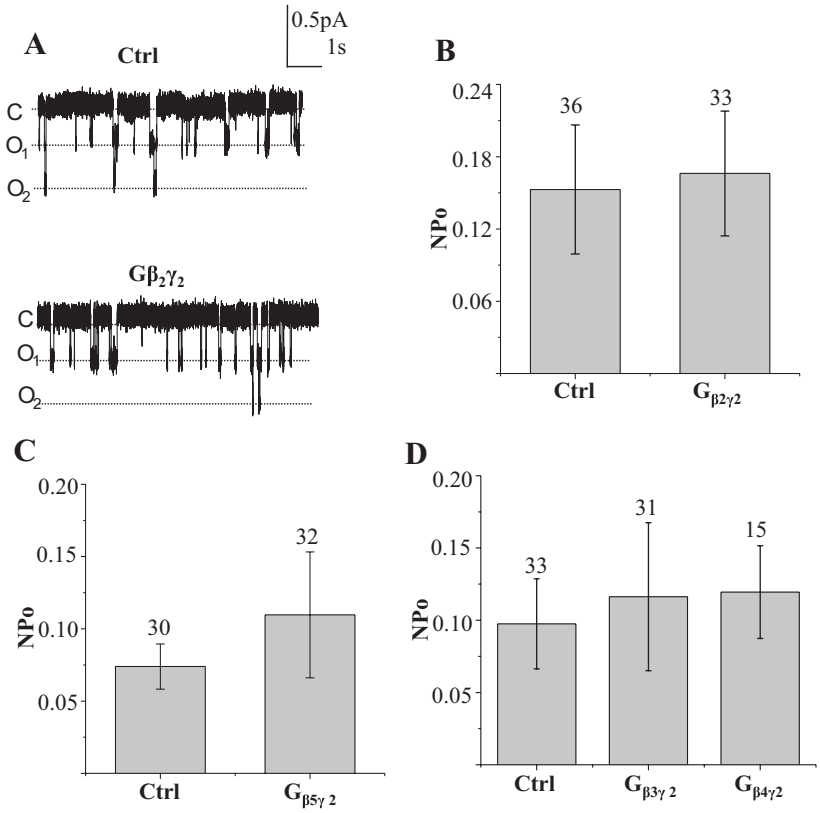

Fig. 3. $G_{\beta 2\gamma 2}$ through $G_{\beta 5\gamma 2}$ have no inhibitory effect on ENaC activity of A6 cells. *A*: representative trace of single-channel records from GFP- and RFP-expressing cells (Control) and $G_{\beta 2\gamma 2}$-expressing cells. The closed state of ENaC is indicated with "c," and channel opening(s) are marked with "o." *B–D*: summary ENaC activity from $G_{\beta 2\gamma 2}$- through $G_{\beta 5\gamma 2}$-expressing cells compared with NP_o of their respective control cells.

the inhibitory effect of $G_{\beta 1\gamma 2}$ on endogenous ENaC of A6 cells is isoform specific, and that the lack of effect of $G_{\beta 2\gamma 2}$–$G_{\beta 5\gamma 2}$ combinations on ENaC in A6 cells is not because of low ENaC activity in particular passages of cells.

A PLC inhibitor blocks $G_{\beta 1\gamma 2}$ inhibition of ENaC activity. In the context of mammalian cellular signaling, all four PLC-β isoforms are activated by the α subunit of G_q, but PLC-β2 and -β3 are also activated by $G_{\beta\gamma}$ subunits (21). To examine whether the inhibitory effect of $G_{\beta 1\gamma 2}$ on ENaC is due to PLC activation in A6 cells (43), we recorded ENaC activity in control and $G_{\beta 1\gamma 2}$-expressing cells after treating the cells with the PLC inhibitor U73122 or its inactive analog U73433 (both 10 μM; IC_{50} = 5 μM) (4) (Fig. 4). In Fig. 4*A*, NP_o of $G_{\beta 1\gamma 2}$-expressing cells treated with U73122 is 0.31 ± 0.11 (n = 27), while NP_o of cells exposed to the inactive analog U73433 is 0.07 ± 0.02 (n = 33), which is significantly lower than the PLC inhibitor-treated cells (P = 0.028). While N of U73433-treated cells is 1.29 ± 0.26 (n = 28), N of U73122-treated cells is 2.59 ± 0.47, (n = 27), which is significantly higher than N of cells treated with the inactive analog (P = 0.017) (Fig. 4*B*). U73122 also restored channel P_o [P_o of U73122-exposed cells is 0.09 ± 0.02 (n = 19), while P_o of U73433-exposed cells is 0.05 ± 0.01 (n = 15), P = 0.049, Fig. 4*C*]. The effect of U73122 is on the $G_{\beta 1\gamma 2}$-induced PLC activity since there was no effect of the inhibitor on control, untransfected cells. In control cells, NP_o, N, and P_o of U73122-

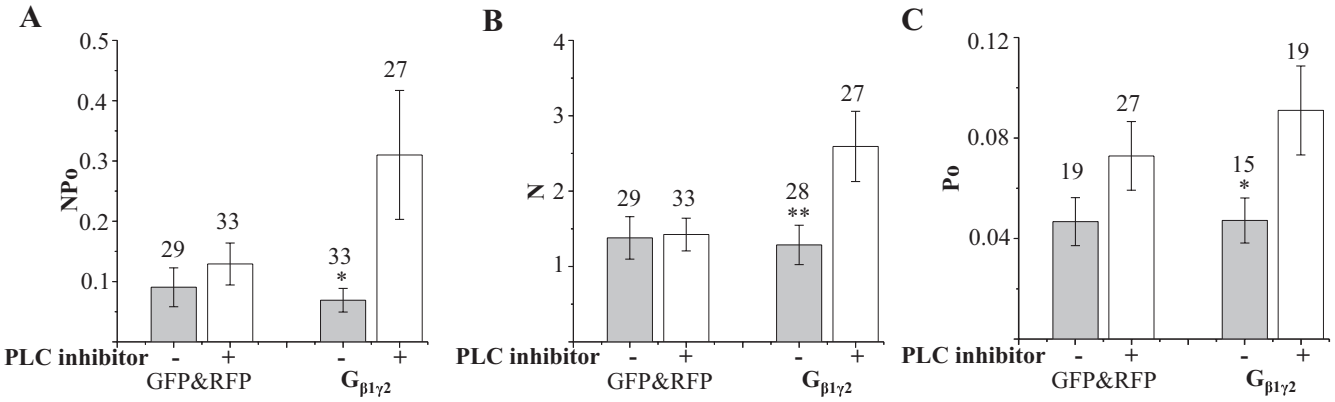

Fig. 4. PLC inhibitor reverses the inhibition of ENaC activity of $G_{\beta 1\gamma 2}$-expressing cells: *A*: ENaC NP_o of control (GFP&RFP) and $G_{\beta 1\gamma 2}$-expressing cells treated with PLC inhibitor U73122 or its inactive analog U73433 (both 10 μM). *B* and *C*: ENaC N and P_o of these cells, respectively. Grey bars are for cells exposed to the inactive analog U73433, indicated as PLC inhibitor (−); open bars are for cells exposed to the inhibitor U73122, indicated as PLC inhibitor (+). The number indicated on top of each column is number of successful patches. Values are means ± SE. *P < 0.05, **P < 0.02.

and U73433-treated cells are not different (NP_o is 0.13 ± 0.03 and 0.09 ± 0.03, Fig. 4*A*, and their N and P_o are 1.42 ± 0.22 vs. 1.38 ± 0.28 and 0.07 ± 0.01 vs. 0.05 ± 0.01, respectively) (Fig. 4, *B* and *C*). That is, in contrast to the significant effect of U73122 on ENaC of $G_{\beta1\gamma2}$-expressing cells, the inhibitor has no significant effect on the channel activity in control, empty vector-expressing cells. These results imply that the activation of PLC contributes to $G_{\beta1\gamma2}$ inhibition of ENaC.

A PKC inhibitor attenuates $G_{\beta1\gamma2}$ suppression of ENaC activity. The above results show that a PLC inhibitor restored both channel N and P_o of $G_{\beta1\gamma2}$-expressing cells. Several previous reports have shown that the primary effect of $PI(4,5)P_2$ does not change the density of functional ENaC on the apical surface but rather alters ENaC P_o (33, 44, 53); therefore, the restoration of ENaC P_o after inhibition of PLC is likely due to maintaining high levels of PIP_2 after prevention of PIP_2 hydrolysis. However, it is unclear whether typical PKC isoforms, which can be activated by PIP_2 hydrolytic products IP_3 and DAG (56), contribute to $G_{\beta1\gamma2}$-induced ENaC inhibition in A6 cells (6, 35, 55). To examine this possibility, we treated $G_{\beta1\gamma2}$-expressing cells and control GFP- and RFP-expressing cells with the PKC inhibitor GF109203x [(IC_{50}) = 360 nM (25)] and compared the channel activity of these cells (Fig. 5). GF109203x (0.4 μM) has no effect on channel activity of control cells (NP_o of treated vs. untreated cells is 0.56 ± 0.2, n = 22, vs. 0.55 ± 0.17, n = 17), but GF109203x significantly reduced the inhibitory effect of $G_{\beta1\gamma2}$ on ENaC activity. In $G_{\beta1\gamma2}$-expressing cells, NP_o in the absence of GF109203x-treated cells is 0.23 ± 0.07 (n = 29), which as expected, is significantly lower than that of control vector-expressing cells, P = 0.05 (Fig. 5*A*, filled column). When $G_{\beta1\gamma2}$-expressing cells were exposed to GF109203x, NP_o increased to 0.50 ± 0.1 (n = 31), which approaches that of control, GFP-, and RFP-expressing cells (Fig. 5*A*, open column). We further examined the effect of the PKC inhibitor on channel N and P_o in $G_{\beta1\gamma2}$-expressing cells. GF109203x increased channel P_o only slightly but significantly restored channel N of $G_{\beta1\gamma2}$-expressing cells (Fig. 5, *B* and *C*); N increased from 1.55 ± 0.35, n = 29, to 2.74 ± 0.42, n = 31, P = 0.03. This result implies that PKC of A6 cells was activated by $G_{\beta1\gamma2}$ overexpression, and this activation resulted in reducing the density of functional channels but has little effect on channel P_o.

ERK1/2 is activated in $G_{\beta1\gamma2}$-expressing cells. In certain cellular contexts, the transient expression of $G_{\beta\gamma}$ heterodimers results in sustained activation of the ERK1/2 kinase cascade (15, 22). The C-terminal tails of β- and γ-ENaC contain ERK1/2 phosphorylation sites (59), and ERK1/2 was reported to participate in EGF- or TGF-α mediated inhibition of amiloride-sensitive transepithelial sodium current in A6 cells and in mouse cortical collecting duct cells (5, 37, 60, 62). To address whether ERK1/2 kinase participates in $G_{\beta1\gamma2}$ inhibition of ENaC in A6 cells, we examined the effects of the kinase inhibitor U0126 (1 μM; IC_{50} = 0.07 μM for MEK 1 and 0.06 μM for MEK 2) (11) on ENaC activity of $G_{\beta1\gamma2}$-expressing cells. In Fig. 6*A*, when $G_{\beta1\gamma2}$-expressing cells were exposed to the vehicle, DMSO, alone, the average NP_o is 0.3 ± 0.07 (n = 22); however, NP_o is significantly increased to 0.75 ± 0.15 (n = 28) ($P < 0.01$) when these cells were treated with U0126. While U0126 has almost no effect on GFP-and RFP-coexpressing cells cultured in parallel, ENaC NP_o of U0126-exposed cells is 0.76 ± 0.17 (n = 22) and for DMSO-exposed cells is 0.72 ± 0.2 (n = 16). Further analyzing channel N and P_o of all these cells, we found that the average N and P_o of GFP- and RFP-expressing cells were not affected by U0126, but U0126 significantly stimulated both N and P_o of $G_{\beta1\gamma2}$-expressing cells. N of cells treated with U0126 vs. the untreated cells is 4 ± 0.5 (n = 28) vs. 2.3 ± 0.07 (n = 22), $P < 0.01$; P_o of treated vs. untreated is 0.17 ± 0.03 (n = 21) vs. 0.11 ± 0.02 (n = 19), $P < 0.01$ (Fig. 6, *C* and *D*). This result indicates that ERK1/2 kinase basal activity is low in unstimulated A6 cells but that it was activated by $G_{\beta1\gamma2}$ expression and this activation inhibits both N and P_o of ENaC.

Substantial literature indicates that $G_{\beta\gamma}$ can induce ERK1/2 activation via PKC-dependent and PKC-independent pathways (20, 48, 56, 58). In the PKC-independent pathway, $G_{\beta\gamma}$ may activate ERK1/2 through PI3K activation (7), or by transactivating other classes of cell surface receptors, such as receptor tyrosine kinases, or integrins at focal adhesion complexes (40, 58). In these PKC-independent mechanisms, Src family nonreceptor tyrosine kinases are usually involved as early intermediates which link $G_{\beta\gamma}$ to activation of the Ras-MAPK pathway (39). To test whether PKC-independent pathways were involved in $G_{\beta1\gamma2}$ activation of ERK1/2, we studied the effect of PI3K and Src kinase inhibitors, respectively, on $G_{\beta1\gamma2}$-mediated ENaC inhibi-

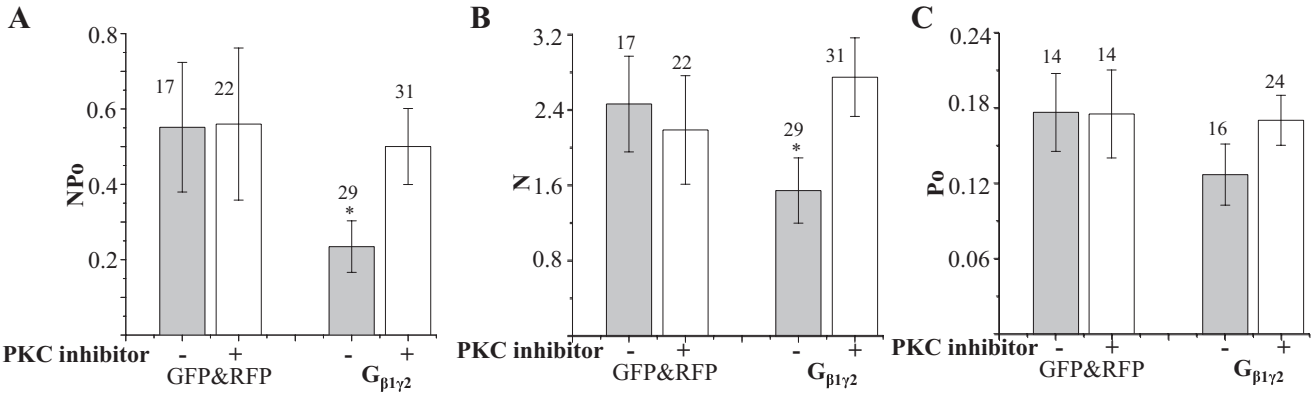

Fig. 5. PKC inhibitor reverses $G_{\beta1\gamma2}$ reduction of ENaC surface expression. *A*: ENaC NP_o of control (GFP&RFP) and $G_{\beta1\gamma2}$-expressing cells exposed to PKC inhibitor GF109203x (0.4 μM) or vehicle (DMSO). *B* and *C*: ENaC N and P_o of these cells. Grey bars are for cells exposed to DMSO, indicated as PKC inhibitor (−); open bars are for cells exposed to GF109203X, indicated as PKC inhibitor (+). The number indicated on top of each column is number of successful patches. Values are means ± SE. *$P < 0.05$.

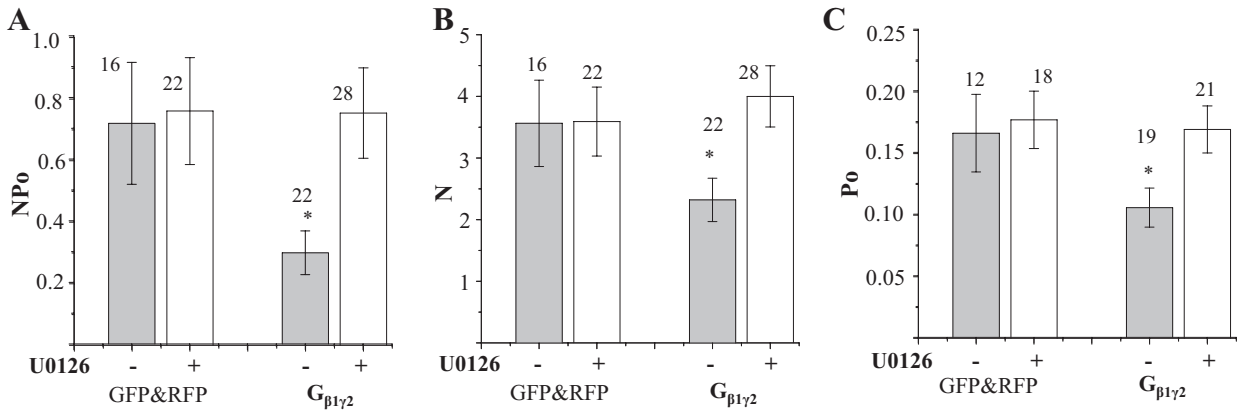

Fig. 6. ERK1/2 inhibitor reverses $G_{\beta1\gamma2}$ inhibition of ENaC activity. *A*: NP_o of control and $G_{\beta1\gamma2}$-expressing cells treated with U0126 (1 μM) or DMSO. *B* and *C*: *N* and P_o of these cells. Grey bars are cells exposed to DMSO, indicated as U0126 (−); open bars are cells exposed to U0126 (+). NP_o, *N*, and P_o of βγ-treated cells are significantly different from all other treatments, but no all other treatments are not different. The number indicated on top of each column is number of successful patches. Values are means ± SE. $^*P < 0.05$.

tion. We first recorded ENaC activity from control or $G_{\beta1\gamma2}$-expressing cells which have been treated with or without PI3K inhibitor LY294002 (10 μM; IC_{50}: 3.8 μM) (63). As the results presented in Fig. 7*A* show, ENaC NP_o of $G_{\beta1\gamma2}$-expressing cells is significantly inhibited in the absence of LY294002 (the grey bars), and this inhibition was partially reversed when these cells were exposed to LY294002 (open bars). In contrast, LY294002 also tends to inhibit ENaC activity in cells expressing GFP and RFP alone, although this inhibition is not significant. The inhibitor of Src family kinases PP2 (10 μM; $IC_{50} = \sim 1$ μM) (38) affects neither ENaC in control cells nor ENaC in $G_{\beta1\gamma2}$-expressing cells (Fig. 8). Therefore, the results of these two sets of experiment imply that neither PI3K nor Src kinases are significantly involved in transferring signaling from $G_{\beta1\gamma2}$ to ERK1/2.

DISCUSSION

Many G protein-coupled receptors have been described in renal epithelial cells and specifically in A6 cells. These include type 2 vasopressin receptors (45), endothelin receptors (16), purinergic receptors (42, 43, 70), prostaglandin receptors (31, 36), dopaminergic receptors (23), and adenosine receptors (41). Descriptions of the physiological effects of G protein activation on ENaC in A6 cells have a long history (1, 2, 9, 10, 50, 54). One initial report showed that the major G protein in the apical membrane of several epithelial cell lines was $G_{i\text{-}3}$ (14). Subsequent work showed that application of $G_{\alpha i\text{-}3}$ to the cytosolic surface of patches excised from the apical membrane activated amiloride-sensitive Na^+ channels (9, 10, 69). The presumption was that somehow the G_α subunit was responsible for the activation; however, at that time the role of βγ subunits was not appreciated. Only later was it shown that application of βγ subunits strongly inhibited ENaC (69). The model that emerged was one in which the primary role of the α subunits was to sequester and, thereby, regulate the levels of βγ, with the βγ subunits being the primary regulators of and interacting partners with ENaC. The βγ subunits achieved this by regulating phospholipase C and PIP_2 levels and by direct interaction with PIP_2 and ENaC.

When we examined A6 cells by real-time PCR, the subunit with the highest level of expression was β1, but we could also detect β4 and low levels of β3 and β5. We were unable to amplify β2. The differences were even more dramatic in Western blots in which we could easily detect β1 but not β2 or β4. Therefore, it seemed that if a subunit were to modify activity in A6 cells it was likely to be β1. However, that β1 was the predominant subunit in A6 cells did not preclude the possibility that other β subunits might also alter ENaC activity.

Using patch-clamp, single-channel recording, we examined different isoforms of G_β subunits in combination with γ2 on

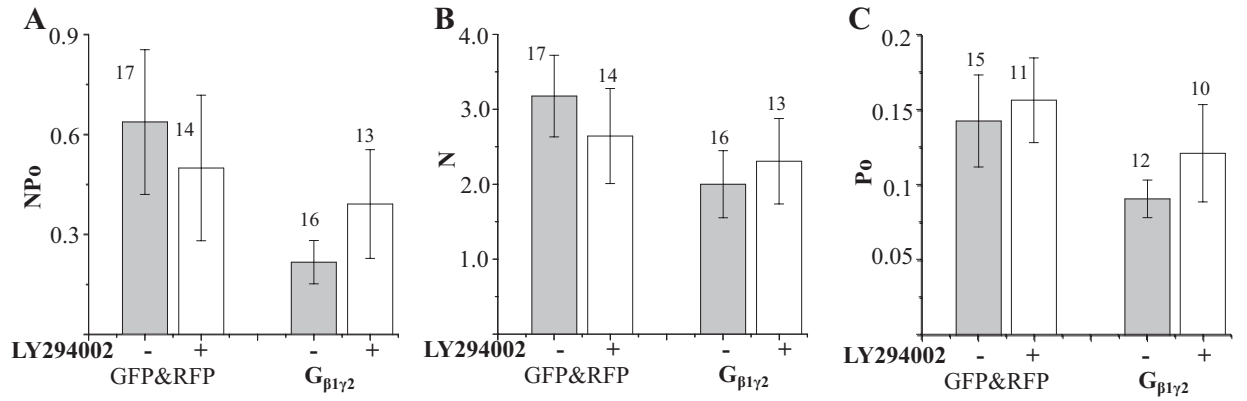

Fig. 7. Effect of a phosphatidylinositol 3-kinase (PI3K) inhibitor on ENaC activity. *A*, *B*, and *C* are the same as in Fig. 6, but cells were treated with the PI3K inhibitor LY294002 (10 μM) or vehicle (DMSO). The inhibitor had no significant effect on βγ inhibition.

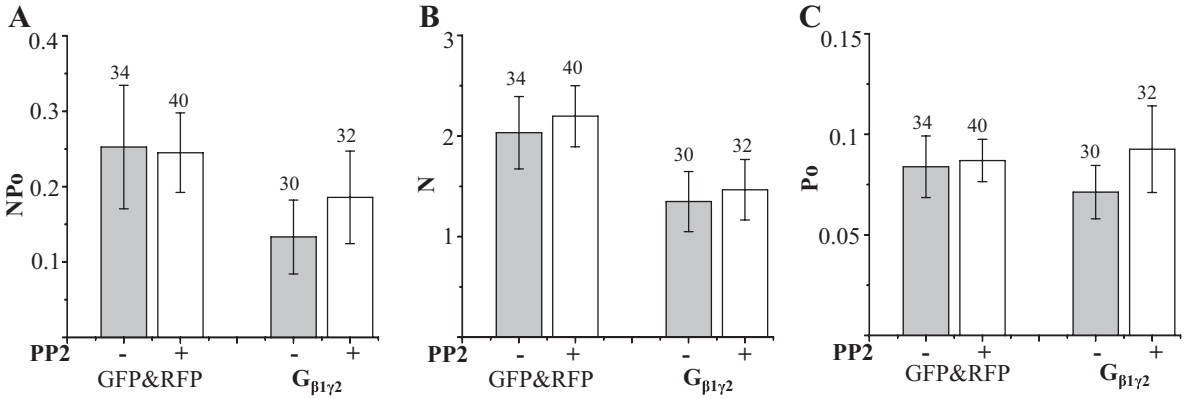

Fig. 8. Effect of Src family kinase inhibitor on ENaC activity. *A*, *B*, and *C* are the same as in Fig. 7, but cells were treated with the Src family kinase inhibitor PP2 (10 μM) or vehicle (DMSO). The inhibitor had no significant effect on βγ inhibition.

endogenous ENaC regulation. Since ENaC activity can vary significantly among different passages or even among cells on different days after confluence, we used cells expressing GFP and RFP alone as a control for each drug treatment to ensure the significance of the results. In this study, we have recorded from >800 patches on A6 cells and found that ENaC activity is significantly inhibited only by the combination of $G_{\beta1\gamma2}$. The inhibitory effect of $G_{\beta1\gamma2}$ is statistically significant in five of six independent experiments, while one did not reach a significant level of inhibition, but this is also the group of cells with the largest variation of ENaC activity among both control and $G_{\beta1\gamma2}$-expressing cells (presented in Fig. 7).

In contrast to the significant effect of $G_{\beta1\gamma2}$, we found the other combinations of dimers from $G_{\beta2\gamma2}$ to $G_{\beta5\gamma2}$ have no significant effect on ENaC regulation. The lack of an inhibitory effect of $G_{\beta2\gamma2}$ through $G_{\beta4\gamma2}$ surprised us because β1 through β4 share >80% identity at an amino acid level (but <50% identity to β5). We repeated $G_{\beta4\gamma2}$ and $G_{\beta5\gamma2}$ combinations in certain passages of A6 cells which have higher endogenous ENaC activity and found again that these two combinations have no effect on ENaC activity. The specific effect of $G_{\beta1\gamma2}$ on ENaC of A6 cells could be due to different G_β isoforms interacting with $G_{\gamma2}$ with different affinities (46), or that $G_{\beta1\gamma2}$ mediates cell type-specific signaling in A6 cells.

In exploring the mechanism of $G_{\beta1\gamma2}$ inhibition of ENaC, we applied several kinase inhibitors to probe signaling pathways that transduce the signal from $G_{\beta1\gamma2}$ to ENaC. The PLC inhibitor U73122 reversed the inhibitory effect of $G_{\beta1\gamma2}$ on ENaC P_o and N (Fig. 3, *B* and *C*). In cells expressing GFP and RFP alone, U73122 tends to increase ENaC P_o but the increase is not significant. Coincidentally, ENaC activity of $G_{\beta1\gamma2}$-expressing cells treated with inactive PLC inhibitor analog U73433 (Fig. 3*A*) is almost identical to that of $G_{\beta1\gamma2}$-expressing cells presented in Fig. 1*B* (both $NP_o = 0.07 \pm 0.02$), and therefore we can compare the results presented in these two figures. U73122 treatment brings the value for *N* of $G_{\beta1\gamma2}$-expressing cells close to that of GFP- and RFP-expressing cells (2.59 ± 0.46 vs. 2.34 ± 1.12) and brings P_o of those cells to 80% of the control level (0.09 ± 0.02 vs. 0.12 ± 0.02). This result implies that PLC basal activity has some effect on ENaC P_o, but that PLC is further activated by $G_{\beta1\gamma2}$ expression, and PLC activation plays a major role in $G_{\beta1\gamma2}$ inhibition of both ENaC *N* and P_o.

Regulation of ENaC *N* and P_o can be fundamentally different: the former mainly depends on channel trafficking and the later on channel gating. However, activated PLC can conceivably produce changes in both *N* and P_o: P_o by reducing plasma membrane PIP_2 levels and *N* by activating PKC as a consequence of PIP_2 hydrolysis. ENaC P_o is influenced by PIP_2 levels (33, 44, 51, 65, 69); however, whether PKC inhibits ENaC surface expression is not completely resolved. Ji et al. (28) reported that several PKC isoforms were involved in SARS virus downregulation of ENaC surface expression. Our result presented in Fig. 5 shows that a PKC inhibitor blocks $G_{\beta1\gamma2}$-mediated ENaC inhibition, and this effect of the inhibitor is mostly due to restoring the channel number in a patch. There are three protein kinase regulatory sites on the C-terminal tails of β and γ subunits of ENaC: casein kinase, PKA/SGK1, and ERK1/2 phosphorylation sites (59); however, a consensus site for PKC on ENaC has never been reported. In fact, attempts to demonstrate direct PKC-mediated ENaC phosphorylation have all been negative (67, 68). Our results suggests that PKC inhibition of ENaC by a $G_{\beta1\gamma2}$-elicited signal is mostly via ERK1/2. This result is consistent with observations reported by Booth and Stockand (3, 6) in which PKC substantially inhibits ENaC activity in A6 cells, and this inhibition is reversed by ERK1/2 inhibitors of U0126 or PD-98059. It is interesting that ENaC activity of $G_{\beta1\gamma2}$-expressing cells is fully reversed when these cells were exposed to an ERK1/2 inhibitor. In Fig. 5*A*, NP_o of $G_{\beta1\gamma2}$-expressing cells is ~40% that of GFP- and RFP-expressing cells, but U0126 treatment brought the NP_o of $G_{\beta1\gamma2}$-expressing cells to almost the same value as that of the control cells. Since our patch-clamp, single-channel recording allows us to resolve ENaC activity into components *N* and P_o, we found that like the PKC inhibitor, U0126 significantly restores ENaC *N* that was suppressed by $G_{\beta1\gamma2}$; but unlike the PKC inhibitor, it also significantly restored ENaC P_o. U0126 stimulates both ENaC *N* and P_o of $G_{\beta1\gamma2}$-expressing cells, implying that the activated ERK1/2 may play dual roles in ENaC regulation. ERK1/2 inhibition of ENaC *N* and P_o was also observed from lung alveolar type II cells when these cells were exposed to strong oxidants (34). The mechanism by which ERK1/2 reduces ENaC surface expression is by ERK1/2 phosphorylation of ENaC, promoting binding of Nedd4-2 to ENaC and thereby enhancing ENaC internalization and degradation (59). How-

ever, the mechanism by which ERK1/2 reduces ENaC P_o is unclear. The ERK1/2-mediated effects on ENaC gating may be due to the following: *1*) ERK1/2 can directly phosphorylate ENaC β, and γ subunits at their C-terminal tails, and this phosphorylation may change the channel conformation and therefore reduce its P_o; *2*) ENaC P_o is enhanced by binding of anionic lipids PIP_2 and PIP_3 (53), and interaction with these negatively charged lipids may be reduced if ENaC is phosphorylated. Interestingly, in mouse collecting duct principle cells, an increase in amiloride-sensitive short-circuit current was observed when U0126 was applied to control cells, indicating a constitutive inhibition of transepithelial Na^+ current by ERK1/2 basal activity (19, 62). However, we did not observe such an increase in our single-channel recording of control cells treated with U0126. A similar result was also reported by Liu et al. (37), who examined the role ERK1/2 in EGF- and TGF-α-induced inhibition of ENaC activity in A6 cells. The lack of a stimulatory effect of U0126 on ENaC activity in control A6 cells may be because *1*) ERK1/2 basal activity is low in these cells; *2*) a transient increase in ENaC activity may have occurred; however, we failed to detect this transient event since our data are the averaged results from cells exposed to U0126 for up to 120 min.

We have also examined the possibility that $G_{\beta1\gamma2}$ activates ERK1/2 through PKC-independent signaling pathways. In those PKC-independent pathways, PI3K and Src family kinases are commonly involved in transferring $G_{\beta\gamma}$ signal to ERK1/2 (29, 39). $G_{\beta\gamma}$ can activate PI3Kγ by interacting directly with the noncatalytic subunit of P101 and therefore promote the catalytic subunit P110 translocation to the plasma membrane (7). The PI3K inhibitor LY294002 applied to $G_{\beta1\gamma2}$-expressing cells tends to restore the ENaC activity of these cells; however, this stimulation is not statistically significant (Fig. 6).

In other experiments, we found that the Src family kinase inhibitor PP2 has no effect on ENaC in either $G_{\beta1\gamma2}$ or GFP- and RFP-expressing cells. Src family kinases contribute at various steps to $G_{\beta\gamma}$ trans-activation of mitogenic signaling pathways (56), but based on our results, we suggest that PKC-independent pathways are not significantly involved in $G_{\beta1\gamma2}$ activation of ERK1/2.

In conclusion, $G_{\beta\gamma}$ inhibition of ENaC activity in A6 cells is G_β isoform specific, and in this cellular context PLC and activation of PKC and ERK1/2 play a major role in transducing $G_{\beta1\gamma2}$ signals to ENaC.

GRANTS

This work was supported by National Institute of Diabetes and Digestive and Kidney Diseases Grant R37 DK037963 to D. C. Eaton.

DISCLOSURES

No conflicts of interest, financial or otherwise, are declared by the authors.

AUTHOR CONTRIBUTIONS

Author contributions: L.Y., O.K.A.-K., B.J.D. performed experiments; L.Y., D.C.E., H.-F.B., O.K.A.-K., B.J.D. analyzed data; L.Y., D.C.E., H.-F.B., interpreted results of experiments; L.Y., B.J.D. prepared figures; L.Y. drafted manuscript; L.Y., D.C.E., H.-F.B., J.D.S., B.J.D. approved final version of manuscript; L.Y., D.C.E., H.-F.B., J.D.S., O.K.A.-K. edited and revised manuscript; L.Y., D.C.E., H.-F.B., J.D.S., provided conception and design of research.

REFERENCES

1. **Ausiello DA, Stow JL, Cantiello HF, De Almeida JB, Benos DJ.** Purified epithelial Na^+ channel complex contains the pertussis toxin-sensitive G alpha i-3 protein. *J Biol Chem* 267: 4759–4765, 1992.
2. **Ausiello DA, Stow JL, Patenaude CR, Cantiello HF.** Guanine nucleotide binding proteins regulate epithelial Na^+ channels. *Adv Exp Med Biol* 290: 333–343, 1991.
3. **Becchetti A, Kemendy AE, Stockand JD, Sariban-Sohraby S, Eaton DC.** Methylation increases the open probability of the epithelial sodium channel in A6 epithelia. *J Biol Chem* 275: 16550–16559, 2000.
4. **Bleasdale JE, Thakur NR, Gremban RS, Bundy GL, Fitzpatrick FA, Smith RJ, Bunting S.** Selective inhibition of receptor-coupled phospholipase C-dependent processes in human platelets and polymorphonuclear neutrophils. *J Pharmacol Exp Ther* 255: 756–768, 1990.
5. **Booth RE, Stockand JD.** Targeted degradation of ENaC in response to PKC activation of the ERK1/2 cascade. *Am J Physiol Renal Physiol* 284: F938–F947, 2003.
6. **Booth RE, Tong Q, Medina J, Snyder PM, Patel P, Stockand JD.** A region directly following the second transmembrane domain in gamma ENaC is required for normal channel gating. *J Biol Chem* 278: 41367–41379, 2003.
7. **Brock C, Schaefer M, Reusch HP, Czupalla C, Michalke M, Spicher K, Schultz G, Nurnberg B.** Roles of G beta gamma in membrane recruitment and activation of p110 gamma/p101 phosphoinositide 3-kinase gamma. *J Cell Biol* 160: 89–99, 2003.
8. **Bugaj V, Pochynyuk O, Stockand JD.** Activation of the epithelial Na^+ channel in the collecting duct by vasopressin contributes to water reabsorption. *Am J Physiol Renal Physiol* 297: F1411–F1418, 2009.
9. **Cantiello HF, Patenaude CR, Ausiello DA.** G protein subunit, $\alpha_{i\text{-}3}$, activates a pertussis toxin-sensitive Na+ channel from the epithelial cell line, A6. *J Biol Chem* 264: 20867–20870, 1989.
10. **Cantiello HF, Patenaude CR, Ausiello DA.** G-protein activation of an epithelial sodium channel is mediated via phospholipid metabolites. *Kidney Int* 37: 213, 1990.
11. **Duncia JV, Santella JB III, Higley CA, Pitts WJ, Wityak J, Frietze WE, Rankin FW, Sun JH, Earl RA, Tabaka AC, Teleha CA, Blom KF, Favata MF, Manos EJ, Daulerio AJ, Stradley DA, Horiuchi K, Copeland RA, Scherle PA, Trzaskos JM, Magolda RL, Trainor GL, Wexler RR, Hobbs FW, Olson RE.** MEK inhibitors: the chemistry and biological activity of U0126, its analogs, and cyclization products. *Bioorg Med Chem Lett* 8: 2839–2844, 1998.
12. **Dupre DJ, Robitaille M, Rebois RV, Hebert TE.** The role of G beta gamma subunits in the organization, assembly, and function of GPCR signaling complexes. *Annu Rev Pharmacol Toxicol* 49: 31–56, 2009.
13. **Ecelbarger CA, Kim GH, Wade JB, Knepper MA.** Regulation of the abundance of renal sodium transporters and channels by vasopressin. *Exp Neurol* 171: 227–234, 2001.
14. **Ercolani L, Stow JL, Boyle JF, Holtzman EJ, Lin H, Grove JR, Ausiello DA.** Membrane localization of the pertussis toxin-sensitive G-protein subunits alpha i-2 and alpha i-3 and expression of a metallothionein-alpha i-2 fusion gene in LLC-PK1 cells. *Proc Natl Acad Sci USA* 87: 4635–4639, 1990.
15. **Faure M, Voynoyasenetskaya TA, Bourne HR.** cAMP and beta-gamma-subunits of heterotrimeric G-proteins stimulate the mitogen-activated protein-kinase pathway in cos-7 cells. *J Biol Chem* 269: 7851–7854, 1994.
16. **Gallego MS, Ling BN.** Regulation of amiloride-sensitive Na^+ channels by endothelin-1 in distal nephron cells. *Am J Physiol Renal Fluid Electrolyte Physiol* 271: F451–F460, 1996.
17. **Garty H, Palmer LG.** Epithelial sodium channels: function, structure, and regulation. *Physiol Rev* 77: 359–396, 1997.
18. **Goldsmith ZG, Dhanasekaran DN.** G protein regulation of MAPK networks. *Oncogene* 26: 3122–3142, 2007.
19. **Grossmann C, Freudinger R, Mildenberger S, Krug AW, Gekle M.** Evidence for epidermal growth factor receptor as negative-feedback control in aldosterone-induced Na^+ reabsorption. 286: F1226–F1231, 2004.
20. **Gutkind JS.** The pathways connecting G protein-coupled receptors to the nucleus through divergent mitogen-activated protein kinase cascades. *J Biol Chem* 273: 1839–1842, 1998.
21. **Harden TK, Sondek J.** Regulation of phospholipase C isozymes by Ras superfamily GTPases. In: *Annual Review of Pharmacology and Toxicology*. Palo Alto, CA: Annual Reviews, 2006, p. 355–379.
22. **Hawes BE, Vanbiesen T, Koch WJ, Luttrell LM, Lefkowitz RJ.** Distinct pathways of G_i-mediated and G_q-mediated mitogen-activated protein-kinase activation. *J Biol Chem* 270: 17148–17153, 1995.
23. **Helms MN, Chen XJ, Ramosevac S, Eaton DC, Jain L.** Dopamine regulation of amiloride-sensitive sodium channels in lung cells. *Am J Physiol Lung Cell Mol Physiol* 290: L710–L722, 2006.
24. **Hepler JR, Gilman AG.** G proteins. *Trends Biochem Sci* 17: 383–387, 1992.

25. **Hers I, Tavare JM, Denton RM.** The protein kinase C inhibitors bisindolylmaleimide I (GF 109203x) and IX (Ro 31-8220) are potent inhibitors of glycogen synthase kinase-3 activity. *FEBS Lett* 460: 433–436, 1999.
26. **Hou YM, Chang V, Capper AB, Taussig R, Gautam N.** G protein beta subunit types differentially interact with a muscarinic receptor but not adenylyl cyclase type II or phospholipase C-beta 2/3. *J Biol Chem* 276: 19982–19988, 2001.
27. **Hwang JI, Fraser IDC, Choi SD, Qin XF, Simon MJ.** Analysis of Ga-mediated chemotaxis by lentiviral delivery of small interfering RNA. *Proc Natl Acad Sci USA* 101: 488–493, 2004.
28. **Ji HL, Song WF, Gao Z, Su XF, Nie HG, Jiang Y, Peng JB, He YX, Liao Y, Zhou YJ, Tousson A, Matalon S.** SARS-CoV proteins decrease levels and activity of human ENaC via activation of distinct PKC isoforms. *Am J Physiol Lung Cell Mol Physiol* 296: L372–L383, 2009.
29. **Kerchner KR, Clay RL, McCleery G, Watson N, McIntire WE, Myung CS, Garrison JC.** Differential sensitivity of phosphatidylinositol 3-kinase p110 gamma to isoforms of G protein beta gamma dimers. *J Biol Chem* 279: 44554–44562, 2004.
30. **Kisselev OG, Ermolaeva MV, Gautam N.** A farnesylated domain in the G-protein gamma-subunit is a specific determinant of receptor coupling. *J Biol Chem* 269: 21399–21402, 1994.
31. **Kokko KE, Matsumoto PS, Zhang ZR, Ling BN, Eaton DC.** Prostaglandin E_2 increases 7-pS Cl^- channel density in the apical membrane of A6 distal nephron cells. *Am J Physiol Cell Physiol* 273: C548–C557, 1997.
32. **Komwatana P, Dinudom A, Young JA, Cook DI.** Cytosolic Na^+ controls an epithelial Na^+ channel via the G(o) guanine nucleotide-binding regulatory protein. *Proc Natl Acad Sci USA* 93: 8107–8111, 1996.
33. **Kunzelmann K, Bachhuber T, Regeer R, Markovich D, Sun J, Schreiber R.** Purinergic inhibition of the epithelial Na^+ transport via hydrolysis of PIP2. *FASEB J* 18: 142, 2004.
34. **Lazrak A, Chen L, Jurkuvenaite A, Doran SF, Liu G, Li Q, Lancaster JR Jr, Matalon S.** Regulation of alveolar epithelial Na^+ channels by ERK1/2 in chlorine-breathing mice. *Am J Respir Cell Mol Biol* 46: 342–354, 2012.
35. **Ling BN, Eaton DC.** Effects of luminal Na^+ on single Na^+ channels in A6 cells, a regulatory role for protein kinase C. *Am J Physiol Renal Fluid Electrolyte Physiol* 256: F1094–F1103, 1989.
36. **Ling BN, Kokko KE, Eaton DC.** Prostaglandin E2 activates clusters of apical Cl^- channels in principal cells via a cyclic adenosine monophosphate-dependent pathway. *J Clin Invest* 93: 829–837, 1994.
37. **Liu L, Duke BJ, Malik B, Yue Q, Eaton DC.** Biphasic regulation of ENaC by TGF-α and EGF in renal epithelial cells. *Am J Physiol Renal Physiol* 296: F1417–F1427, 2009.
38. **Lu R, Alioua A, Kumar Y, Kundu P, Eghbali M, Weisstaub NV, Gingrich JA, Stefani E, Toro L.** c-Src tyrosine kinase, a critical component for 5-HT2A receptor-mediated contraction in rat aorta. *J Physiol* 586: 3855–3869, 2008.
39. **Luttrell DK, Luttrell LM.** Not so strange bedfellows: G-protein-coupled receptors and Src family kinases. *Oncogene* 23: 7969–7978, 2004.
40. **Luttrell LM.** 'Location, location, location': activation and targeting of MAP kinases by G protein-coupled receptors. *J Mol Endocrinol* 30: 117–126, 2003.
41. **Ma H, Ling BN.** Luminal adenosine receptors regulate amiloride-sensitive Na^+ channels in A6 distal nephron cells. *Am J Physiol Renal Fluid Electrolyte Physiol* 270: F798–F805, 1996.
42. **Ma HP, Bao HF, Liang YY, Kemp MJ, Malik B, Ling BN, Eaton DC.** ATP inhibits ENaC via both PIP, and PKC. In: 36th Annual Meeting of the American Society of Nephrology in San Diego, CA. 14: 81A–82A, 2003.
43. **Ma HP, Li L, Zhou ZH, Eaton DC, Warnock DG.** ATP masks stretch activation of epithelial sodium channels in A6 distal nephron cells. *Am J Physiol Renal Physiol* 282: F501–F505, 2002.
44. **Ma HP, Saxena S, Warnock DG.** Anionic phospholipids regulate native and expressed epithelial sodium channel (ENaC). *JBC* 277: 7641–7644, 2002.
45. **Marunaka Y, Eaton DC.** Effects of vasopressin and cAMP on single amiloride-blockable Na channels. *Am J Physiol Cell Physiol* 260: C1071–C1084, 1991.
46. **McIntire WE.** Structural determinants involved in the formation and activation of G protein beta gamma dimers. *Neurosignals* 17: 82–99, 2009.
47. **McIntire WE, MacCleery G, Garrison JC.** The G protein beta subunit is a determinant in the coupling of G_s to the $beta_1$-adrenergic and A2a adenosine receptors. *J Biol Chem* 276: 15801–15809, 2001.
48. **Miller WE, Lefkowitz RJ.** Expanding roles for beta-arrestins as scaffolds and adapters in GPCR signaling and trafficking. *Curr Opin Cell Biol* 13: 139–145, 2001.
49. **Myung CS, Lim WK, DeFilippo JM, Yasuda H, Neubig RR, Garrison JC.** Regions in the G protein gamma subunit important for interaction with receptors and effectors. *Mol Pharmacol* 69: 877–887, 2006.
50. **Ohara A, Matsunaga H, Eaton DC.** G-protein activation inhibits amiloride-blockable highly selective sodium channels in A6 cells. *Am J Physiol Cell Physiol* 264: C352–C360, 1993.
51. **Pochynyuk O, Bugaj V, Rieg T, Insel PA, Mironova E, Vallon V, Stockand JD.** Paracrine regulation of the epithelial Na^+ channel in the mammalian collecting duct by purinergic $P2Y_2$ receptor tone. *J Biol Chem* 283: 36599–36607, 2008.
52. **Pochynyuk O, Rieg T, Bugaj V, Schroth J, Fridman A, Boss GR, Insel PA, Stockand JD, Vallon V.** Dietary Na^+ inhibits the open probability of the epithelial sodium channel in the kidney by enhancing apical $P2Y_2$-receptor tone. *FASEB J* 24: 2056–2065.
53. **Pochynyuk O, Tong QS, Medina J, Vandewalle A, Staruschenko A, Bugaj V, Stockand JD.** Molecular determinants of PI(4,5)P-2 and PI(3,4,5)P-3 regulation of the epithelial Na^+ channel. *J Gen Physiol* 130: 399–413, 2007.
54. **Rokaw MD, Benos DJ, Palevsky PM, Cunningham SA, West ME, Johnson JP.** Regulation of a sodium channel-associated G-protein by aldosterone. *J Biol Chem* 271: 4491–4496, 1996.
55. **Rokaw MD, West M, Johnson JP.** Rapamycin inhibits protein kinase C activity and stimulates Na^+ transport in A6 cells. *J Biol Chem* 271: 32468–32473, 1996.
56. **Rozengurt E.** Mitogenic signaling pathways induced by G protein-coupled receptors. *J Cell Physiol* 213: 589–602, 2007.
57. **Schild L.** The epithelial sodium channel: from molecule to disease. In: *Reviews of Physiology, Biochemistry and Pharmacology*. New York: Springer, 2004, p. 93–107.
58. **Schwindinger WF, Robishaw JD.** Heterotrimeric G-protein beta gamma-dimers in growth and differentiation. *Oncogene* 20: 1653–1660, 2001.
59. **Shi HK, Asher C, Chigaev A, Yung Y, Reuveny E, Seger R, Garty H.** Interactions of beta and gamma ENaC with Nedd4 can be facilitated by an ERK-mediated phosphorylation. *J Biol Chem* 277: 13539–13547, 2002.
60. **Taruno A, Niisato N, Marunaka Y.** Hypotonicity stimulates renal epithelial sodium transport by activating JNK via receptor tyrosine kinases. *Am J Physiol Renal Physiol* 293: F128–F138, 2007.
61. **Tong QS, Stockand JD.** Receptor tyrosine kinases mediate epithelial Na^+ channel inhibition by epidermal growth factor. *Am J Physiol Renal Physiol* 288: F150–F161, 2005.
62. **Veizis IE, Cotton CU.** Abnormal EGF-dependent regulation of sodium absorption in ARPKD collecting duct cells. *Am J Physiol Renal Physiol* 288: F474–F482, 2005.
63. **Vlahos CJ, Matter WF, Hui KY, Brown RF.** A specific inhibitor of phosphatidylinositol 3-kinase, 2-(4-morpholinyl)-8-phenyl-4H-1-benzopyran-4-one (LY294002). *J Biol Chem* 269: 5241–5248, 1994.
64. **Watson AJ, Katz A, Simon MI.** A 5th member of the mammalian g-protein beta-subunit family—expression in brain and activation of the beta-2 isotype of phospholipase-C. *JBC* 269: 22150–22156, 1994.
65. **Weixel KM, Edinger RS, Kester L, Guerriero CJ, Wang HM, Fang L, Kleyman TR, Welling PA, Weisz OA, Johnson JP.** Phosphatidylinositol 4-phosphate 5-kinase reduces cell surface expression of the epithelial sodium channel (ENaC) in cultured collecting duct cells. *J Biol Chem* 282: 36534–36542, 2007.
66. **Yu L, Eaton DC, Helms MN.** Effect of divalent heavy metals on epithelial Na^+ channels in A6 cells. *Am J Physiol Renal Physiol* 293: F236–F244, 2007.
67. **Yue G, Eaton DC.** Protein kinase C does not affect epithelial Na^+ channel activity in A6 cells with inside-out patch clamp study. *FASEB J* 12: 1042, 1998.
68. **Yue G, Edinger RS, Bao HF, Johnson JP, Eaton DC.** The effect of rapamycin on single ENaC channel activity and phosphorylation in A6 cells. *Am J Physiol Cell Physiol* 279: C81–C88, 2000.
69. **Yue G, Malik B, Eaton DC.** Phosphatidylinositol 4,5-bisphosphate (PIP2) stimulates epithelial sodium channel activity in A6 cells. *J Biol Chem* 277: 11965–11969, 2002.
70. **Zhang Y, Sanchez D, Gorelik J, Klenerman D, Lab M, Edwards C, Korchev Y.** Basolateral P2X4-like receptors regulate the extracellular ATP-stimulated epithelial Na^+ channel activity in renal epithelia. *Am J Physiol Renal Physiol* 292: F1734–F1740, 2007.